



Nuclear magnetic resonance immunoassay of tetanus antibodies based on the displacement of magnetic nanoparticles

Pavel Khramtsov¹ · Maria Kropaneva¹ · Maria Bochkova¹ · Dmitriy Kiselkov² · Valeria Timganova¹ · Svetlana Zamorina¹ · Mikhail Rayev¹

Received: 29 October 2019 / Revised: 11 November 2020 / Accepted: 3 December 2020 / Published online: 25 January 2021
© Springer-Verlag GmbH Germany, part of Springer Nature 2021

Abstract

A nuclear magnetic resonance (NMR) immunoassay based on the application of carbon-coated iron nanoparticles conjugated with recognition molecules was designed. The principle of the assay is that ELISA plates are coated with a capture element, and then an analyte is added and detected by conjugating the magnetic nanoparticles with recognition molecules. Afterwards, the elution solution (0.1-M sodium hydroxide) is added to displace the magnetic nanoparticles from the well surfaces into the solution. The detached magnetic nanoparticles reduce transverse relaxation time (T₂) values of protons from the surrounding solution. A portable NMR relaxometer is used to measure the T₂. Magnetic nanoparticles conjugated with streptavidin, monoclonal antibodies, and protein G were applied for the detection of biotinylated albumin, prostate-specific antigen, and IgG specific to tetanus toxoid (TT). The limit of detection of anti-TT IgG was 0.08–0.12 mIU/mL. The reproducibility of the assay was within the acceptable range (CV < 7.4%). The key novelty of the immunoassay is that the displacement of the nanoparticles from the solid support by the elution solution allows the advantages of the solid phase assay to be combined with the sensitive detection of the T₂ changes in a volume of liquid.

Keywords Relaxometry · Elution · Assay · Magnetic nanoparticles

Introduction

Magnetic nanoparticles are widely used as reporter probes in biosensing due to their ability to generate different magnetic signals. The most notable magnetic nanoparticle application is detecting viruses, bacteria, tumor cells, proteins, DNA, RNA, ions, and amino acids [1, 2]. There are numerous sensing platforms based on different magnetic effects: anisotropic magnetoresistance, giant magnetoresistance, tunneling magnetoresistance, magnetic relaxation (used by superconducting quantum interference devices (SQUIDs)), remanence or

alternating current susceptibility, giant magnetoimpedance, the Hall effect, and nuclear magnetic resonance (NMR) [3–7].

NMR-based biosensing platforms rely on magnetic nanomaterials' ability to change the longitudinal relaxation time (T₁) or transverse relaxation time (T₂) of the surrounding water protons. Most of these assays are homogeneous [8] and thus performed in the liquid volume. The critical event that occurs during analysis is the clustering (or declustering) of magnetic nano- or microparticles upon the addition of an analyte of interest. Single particles and clusters have different relaxivities (i.e., their ability to change the T₁ or T₂). Therefore, the concentration of the analyte can be calculated by measuring the relaxation time. This type of analysis is called magnetic relaxation switches.

Despite being faster and simpler, homogeneous assays have, as a rule, lower sensitivity, and specificity because of the absence of washing steps [9]. Although NMR relaxometry is typically a method of analysis in liquid volume, several advances in the development of heterogeneous (solid phase) NMR assays have been made. Burtea et al. [10] performed an ELISA-like assay, using iron oxide nanoparticles as labels. Magnetic resonance imaging was applied to detect and

✉ Pavel Khramtsov
khrantsov Pavel@yandex.ru

¹ Institute of Ecology and Genetics of Microorganisms, Perm Federal Research Center of the Ural Branch of the Russian Academy of Sciences, 13 Golev Str., Perm 614081, Russia

² Institute of Technical Chemistry, Perm Federal Research Center of the Ural Branch of the Russian Academy of Sciences, 3 Academician Korolev Str., Perm 614013, Russia

quantify the magnetic nanoparticles attached to the well surfaces. In our previous works, we developed a dot blot NMR immunoassay to detect prostate-specific antigen (PSA) and IgG against tetanus toxoid using carbon-coated iron nanoparticles conjugated with monoclonal antibodies or Streptococcal protein G [11, 12]. We applied a custom-made portable NMR relaxometer to measure the protons' transverse relaxation time inside the porous membrane. These analyses were sensitive enough to measure clinically relevant concentrations of PSA and IgG. The disadvantages of dot blot NMR immunoassay include the small volume of nitrocellulose test strips, which contained too few water molecules (and, consequently, protons) available for interaction with magnetic nanoclusters. Besides, when analyzing a large number of samples, processing multiple test strips is time-consuming.

This study aimed to develop a more convenient NMR assay with improved sensitivity. To achieve this goal, we needed to increase the number of water molecules available for interaction with magnetic nanoparticles. We assumed that if the analysis is performed in a standard 96-well plate, immune complexes containing magnetic nanoparticles are formed on the wells' surface. In this case, the nanoparticles will only decrease the T2 of protons located in the wells' surface vicinity. In order to increase the number of available protons, we destroyed immune complexes using various elution solutions. In this case, the nanoparticles break off from the well's walls and float freely in the volume of the elution solution, which leads to a significant increase in the available protons, and therefore to an increase in T2. This approach allowed us to combine the advantages of conventional solid-phase analyses with the advantages of NMR assay in a liquid volume.

Currently, several analyses based on the displacement of nanoparticles from the solid phase have been developed. The competitive elution of fluorescent nanoparticles [13] or Au nanoparticles (detected by anodic stripping voltammetry) [14] was used for the quantification of free biotin. An enzyme-mediated detachment of gold nanoparticles with microscopic detection was employed to determine nucleases' activity [15]. The electrochemical detection of aflatoxin was conducted by displacing antibody-coated silica nanoparticles with free aflatoxin from the electrode surface [16]. The elution of Au nanoparticles functionalized with lactosyl-PEG from an SPR sensor was used to detect galactose [17]. Besides, elution is a common step performed during affine isolation and the purification of biomolecules.

In this work, we present a novel indirect NMR immunoassay of anti-tetanus IgG in 96-well plates (Fig. 1). Wells were coated with tetanus toxoid; then, serum samples or calibrators were added. Bound antibodies were detected by Streptococcal protein G conjugated with magnetic nanoparticles. The subsequent addition of an elution solution led to the displacement of the magnetic nanoparticles from the well surfaces into the solution. The magnetic nanoparticles reduced the T2 of the

protons in the elution solution. Relaxation time was measured by a portable NMR relaxometer.

The essential advantage of this approach is that the magnetic nanoparticles that were freely distributed in the solution affected the relaxation times of more protons compared with nanoparticles attached to the wells' surface. It endows the assay with higher sensitivity and better resolution compared to NMR assay on a porous membrane. Besides, magnetic nanoparticles have some advantages over traditional enzyme tags (particularly horseradish peroxidases), namely, thermal stability, resistance to peroxidase inhibitors, such as sodium azide, and cysteine, and heavy metal cations.

Materials and methods

Materials

Polystyrene ELISA plates with high protein binding were obtained from SPL (China). Bovine serum albumin was obtained from Amresco (USA). Biotin N-hydroxysuccinimide ester, casein, and human IgG were obtained from Sigma-Aldrich (USA). Sodium azide, urea, potassium thiocyanate, sodium hydroxide, sodium chloride, sodium hydrogen phosphate, sodium dihydrogen phosphate, and Tween-20 were obtained from ITW Reagents (USA). Hydrochloric acid was obtained from Reakhim (Russia). PSA and anti-PSA monoclonal antibodies (clones 3A6 and 1A6) were obtained from Bialexa (Russia). Streptavidin was obtained from ProspecBio (Israel). Recombinant protein G obtained from *Streptococcus sp.* was kindly provided by Dr. Tatyana Gupalova of the Institute of Experimental Medicine (St. Petersburg, Russia). Tetanus toxoid was obtained from Mikrogen (Russia). WHO standard of anti-tetanus IgG (TE-3) was obtained from NIBSC (UK). Tetanus IgG ELISA kit was obtained from Virion/Serion (Germany).

Blood serum samples were obtained from 14 volunteers vaccinated against tetanus and one non-vaccinated volunteer. Sera from three intact rabbits were obtained from Mikrogen (Russia) and pooled. The serum samples were stored at $-20\text{ }^{\circ}\text{C}$. No anti-tetanus antibodies were detected in pooled rabbit serum by ELISA.

The following buffers were used: a 0.2-M carbonate buffer with a pH of 9.6, phosphate buffer (PB, 0.15-M NaCl, 0.015-M Na_2HPO_4 , 0.015-M NaH_2PO_4 , and 0.1% NaN_3 , pH = 7.25), and PBT (PB + 0.1% Tween-20).

The following instrumentation was used: a Stat Fax 2600 microplate washer (Awareness Technology, USA), Multiskan Sky UV-Vis Reader (Thermo, USA) and ZetaSizer NanoZS particle analyzer (Malvern, UK), scanning electron microscope FEI Quanta 650FEG equipped with EDAX Octane Elite detector (Thermo, USA).

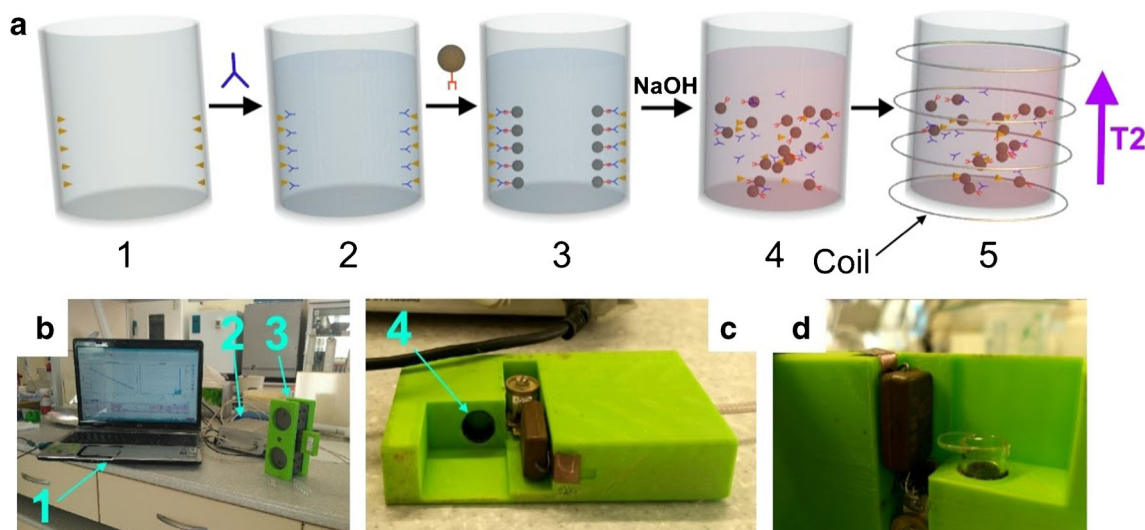


Fig. 1 **a** Scheme of anti-TT IgG assay: 1, coating of the wells with TT (yellow triangles); 2, the addition of sample containing anti-TT IgG; 3, the addition of magnetic nanoparticles conjugated with Streptococcal protein G; 4, the addition of elution solution (0.1-M NaOH); 5,

measurement of T2. **b** NMR measurement setup. **c** Relaxometer and sample holder. **d** Well loaded with the sample inside the radiofrequency coil of the holder. 1, laptop; 2, portable relaxometer; 3, sample holder inside the magnet; 4, radiofrequency coil

Preparation of the conjugates

The carbon-coated iron nanoparticles were aminated, covered with a BSA layer, and coupled with protein G (Fe@C-NH₂/BSA/G), streptavidin (Fe@C-NH₂/BSA/Str), and MAbs specific to PSA (Fe@C-NH₂/BSA/MAb), as described in [12]. Properties of these nanoparticles were previously characterized in detail [12].

Stability of the nanoconjugates in the elution solutions

Fe@C-NH₂/BSA/G was diluted 1:350 (final concentration 2.8 μg/mL) in 750 μL of PB, 0.1-M HCl, 3-M KSCN, 8-M urea, or 0.1-M NaOH (3 samples for each solvent). The hydrodynamic diameter was measured immediately after dilution and then after 1 and 2 h. The solutions were kept at room temperature throughout the experiment. The solvent parameters were as follows: the viscosity and refractive index of the 8-M urea solution at 25 °C were 1.6270 cPa and 1.400, respectively, and the viscosity and refractive index of the 3-M KSCN solution at 25 °C were 0.8861 cPa and 1.390 [18–20]. The viscosity and refractive index of PB, 0.1-M HCl, and 0.1-M NaOH solutions were considered equal to that of water. Measurement was performed in auto mode. Intensity-weighted size distributions are reported throughout the article.

Measurement of the relaxation times

A custom-made NMR relaxometer was used for the NMR assay. Relaxometer was developed in the Lab of Applied Magnetism, M.N. Mikheev Institute of Metal Physics,

Yekaterinburg, Russia. The magnet assembly of the device was based on permanent SmCo magnets with a field of ~ 2 kOe (0.2 T) and heterogeneity of no more than 3×10^{-5} in the sample volume (1 cm³), which provides a measuring frequency of approximately 7.75 MHz. To compensate for the temperature drift of the field before the measurement, the device's reference frequency was adjusted with an accuracy of 10 Hz to the Larmor resonance frequency of the water protons in the sample.

The device was based on the Analog Devices BF-937 DSP processor. The device communicated with a computer via a USB connector; custom-made software was used to interact with the PC, through which the device was controlled. The same software was used to mathematically process the results, including the calculation of the relaxation times.

The measuring unit was inserted into the magnet assembly of the NMR relaxometer and consisted of a radio frequency coil (RF coil) and a few capacitors in a 3D-printed plastic (PLA) case. For the T₂ measurement, single wells were placed inside the RF coil; then, the measuring unit was inserted inside the magnet's hole.

The results of the measurements are expressed as the ratio of the T₂ of 100 μL of the tested sample and the T₂ of 100 μL of pure elution solution (T_{2T}/T_{2E}).

Assay procedure: direct detection of IgG

One hundred microliters of human IgG was diluted tenfold with a 0.2-M carbonate buffer with a pH of 9.6, and the resulting solution was added into the wells of a polystyrene plate. The coating was performed for 2 h. The wells were washed three times with 250 μL of PBT using a microplate washer, and then

200 μL of a blocking buffer (PBT + 2% casein + 1% BSA) was added. The plates were maintained for 1 h and washed. The Fe@C-NH₂/BSA/G suspension (100 μL , 0.05 mg/mL) in PBT + 2% casein was added and reacted for 60 min. After washing, 100 μL of the elution solutions was added. The relaxation times of the protons were measured in each well after 1 h. Single wells were broken off and placed inside the coil of the relaxometer. All the assay steps except for the washing and measurement steps were performed at 37 °C.

Assay procedure: direct detection of biotinylated BSA

One hundred microliters of biotinylated BSA Bi-BSA was diluted tenfold with a 0.2-M carbonate buffer with a pH of 9.6, and the resulting solution was added into the wells of a polystyrene plate. The coating was performed for 2 h. The wells were washed three times with 250 μL of PBT using a microplate washer, and then 200 μL of a blocking buffer (PBT + 2% casein + 1% BSA) was added. The plates were maintained for 1 h and washed. The Fe@C-NH₂/BSA/Str suspension (100 μL , 0.05 mg/mL) in PBT + 2% casein was added and reacted for 60 min. After washing, 100 μL of the elution solutions was added. The relaxation times of the protons were measured in each well after 1 h. Single wells were broken off and placed inside the coil of the relaxometer. All the assay steps except for the washing and measurement steps were performed at 37 °C.

Assay procedure: sandwich analysis of PSA

One hundred microliters of mouse anti-PSA IgG (clone 3A6) was diluted to 0.05 mg/mL in a 0.2-M carbonate buffer with a pH of 9.6, and the resulting solution was added into the wells of a polystyrene plate. The coating was performed for 2 h. The wells were washed three times with 250 μL of PBT using a microplate washer, and then 200 μL of a blocking buffer (PBT + 2% casein + 1% BSA) was added. The plates were maintained for 1 h and washed. One hundred microliters of PSA diluted tenfold in the blocking buffer was added and incubated for 1 h; the wells were washed. The Fe@C-NH₂/BSA/Mab suspension (100 μL , 0.05 mg/mL) in PBT + 2% casein was added and reacted for 60 min. After washing, 100 μL of the elution solutions was added. The relaxation times of the protons were measured in each well after 1 h. Single wells were broken off and placed inside the coil of the relaxometer. All the assay steps except for the washing and measurement steps were performed at 37 °C.

Assay procedure: indirect detection of anti-tetanus toxoid IgG

One hundred microliters of tetanus toxoid were diluted to 0.05 mg/mL in a 0.2-M carbonate buffer with a pH of 9.6,

and the resulting solution was added into the wells of a polystyrene plate. The coating was performed for 2 h. The wells were washed three times with 250 μL of PBT using a microplate washer, and then 200 μL of a blocking buffer (PBT + 2% casein + 1% BSA) was added. The plates were maintained for 1 h and washed. Calibrators or serum samples (100 μL) were added to the wells and incubated for 1 h; the wells were washed. The Fe@C-NH₂/BSA/G suspension (100 μL , 0.05 mg/mL) in PBT + 2% casein was added and reacted for 60 min. After washing, 100 μL of 0.1-M NaOH was added. The relaxation times of the protons were measured in each well after 1 h. Single wells were broken off and placed inside the coil of the relaxometer. All the assay steps except for the washing and measurement steps were performed at 37 °C.

Calibrators were prepared as follows. Anti-tetanus toxoid (TT) IgG was fourfold diluted in the blocking buffer, which contained 1% of rabbit serum. Final concentration of IgG in calibrators was 100, 25, 6.25, 1.56, 0.39, 0.097, 0.024, and 0 mIU/mL. Three technical replicates of each calibrator were analyzed to obtain the calibration curve. Rabbit blood serum was used as a matrix because we could not get enough human serum that does not contain antibodies to tetanus because of the high population immunity to tetanus in Russia.

The lower limit of detection (LOD) was determined as concentration corresponding to the mean T_{2T}/T_{2E} of a blank sample + 3 \times standard deviation.

The spike-recovery test (accuracy) and reproducibility test (precision) were performed using the same samples prepared as follows. Whole rabbit blood serum was spiked with different anti-TT IgG amounts to obtain a wide range of concentrations: 80, 50, 10, 5, 3, 2, 1.3, and 0.2 mIU/ml (from low to high). The concentration of anti-TT IgG in TE-3 standard is 130 IU/mL; therefore, it was preliminarily diluted in PB when samples with low concentrations were prepared. Ten technical replicates of each spiked sample were tested simultaneously. Concentrations of IgG were back-calculated from the calibration curve. Mean concentration was obtained for each spiked sample and compared with expected concentration value:

$$\text{recovery} = \frac{\text{observed concentration}}{\text{expected concentration}} \times 100\%$$

Reproducibility was expressed as coefficient of variation (CV), i.e., the ratio between standard deviation and mean observed concentration (from 10 replicates):

$$\text{CV} = \frac{\text{standard deviation}}{\text{mean concentration}} \times 100\%$$

Fifteen blood serum samples were tested using ELISA and NMR analysis; after which, we compared the results. To do this, we used the Bland-Altman method.

Scanning electron microscopy and energy dispersive spectroscopy elemental analysis of positive and negative eluted samples

Twenty-four positive (100 mIU/mL of anti-TT IgG) and twenty-four negative (0 mIU/mL) samples were analyzed as described in the section “[Assay procedure: indirect detection of anti-tetanus toxoid IgG.](#)” After T2 measurements, elution solutions were combined; the resulting total volume of positive and negative samples was 2.4 mL. They were further dialyzed against deionized water, transferred into plastic tubes, and concentrated at 95 °C in the oven to 100–200 µL. Concentrated samples were applied in portions of 10 µL onto silicon wafers (5 × 5 mm). After the application of each portion, the wafers were dried under vacuum and analyzed by SEM.

The detection of magnetic nanoparticles in samples was carried out using field emission scanning electron microscope FEI Quanta 650FEG and an EDAX Octane Elite detector for energy dispersive X-ray spectroscopy (EDS). The dialyzed solution was drop-cast on a silicon substrate using a micropipette and dried under vacuum; the procedure was repeated several times until the whole solution was deposited. The area of 188 × 148 µm was analyzed using EDS at 5 kV; the map that contained 1000 × 800 spectra were recorded and analyzed using the “create max pixel spectrum” procedure of EDAX Team software that is used for searching small inclusions or particles when their contribution to the sum spectrum is too low.

Data analysis

The acquired data were processed in MS Office Excel, Microsoft (USA). The graphs were prepared in GraphPad Prism 6.01, GraphPad Inc. (USA). The curve fitting was performed in Origin 2020b, OriginLab Corporation (USA).

The NMR analysis data were adjusted to a four-parameter logistic model, which is traditionally used for fitting symmetrical sigmoidal dose-response curves in immunoassays (1/Y² residual weighting scheme was applied). The general equation of the logistic function is:

$$y = A_2 + \frac{(A_1 - A_2)}{(1 + (x/x_0)^p)}$$

Results and discussion

Optimization of elution conditions

There are many ways to split antibody-protein G and antibody-antigen pairs: changing the pH, ionic strength, or

temperature and adding chaotropic agents [21]. In affinity chromatography, the elution conditions should be as mild as possible, because the retention of the functional activity of a protein of interest is necessary. In contrast, we did not attempt to reuse the eluted nanoparticles but rather needed the reagent capable of rapidly detaching and providing colloidal stability to the nanoparticles. According to the literature, IgG can be efficiently eluted from a protein G column at a pH ~ 1–2 [22]. Acevedo et al. [23] demonstrated that 3-M KSCN, a Tris buffer with a pH of 11.6 and 8-M urea, detached 80–90% of the monoclonal antibodies produced by different hybridomas from an affinity column. The most straightforward approach is using solutions with extreme pH values. It is known that BSA-coated nanoparticles had a good colloidal stability in neutral and alkaline buffers, but the nanoparticles precipitated in acidic conditions at pH values close to the pI of BSA [12, 24, 25].

In this work, we used a PB (control), 0.1-M HCl, 0.1-M NaOH, 8-M urea, and 3-M KSCN as the elution solutions. Nanoparticles must be stable in an eluent, because aggregated nanoparticles have a much lower relaxivity and sediment on the bottom of the well, resulting in a low sensitivity and bad reproducibility. The Fe@C-NH₂/BSA/G particles were stable in all the studied elution solutions for 2 h at room temperature (Fig. 2a). Therefore, efficiency of all diluents was further tested. First, the direct analysis of human IgG and the sandwich analysis of PSA were performed. The wells were loaded with the elution solutions and agitated for 60 min. The resolution and sensitivity of the assays were almost the same for all tested elution solutions (Fig. 2b, c). As expected, an insignificant change in the T2 was observed when the PB was added to the wells, confirming that the nanoparticles attached to the well surfaces affected the relaxivity of few protons. In contrast, detached nanoparticles that are freely distributed in the volume of the eluent strongly decrease the T2.

Biotinylated proteins are widely used in immunoassays to enhance the analytical signal, and the most common approach is labeling secondary antibodies with biotin in sandwich assays. The bond between streptavidin and biotin is one of the strongest noncovalent bonds found in nature. Usually, harsh elution conditions and the addition of free biotin are necessary to disrupt the bond between biotin and streptavidin [26]. Detachment solutions used to split “protein G-IgG” and “IgG-PSA” pairs are unable to disrupt the bond between streptavidin and biotin. However, we suggested that they can cause proteins to desorb from the walls of the polystyrene plate, displacing the “Bi-BSA + nanoparticle” complexes. We coated the polystyrene plates with serially diluted biotinylated BSA; Bi-BSA was detected by Fe@C-NH₂/BSA/Str. Only 0.1-M NaOH efficiently detached the magnetic nanoclusters, whereas a negligible change in the T2 was observed when other eluents were used (Fig. 2d). The resulting calibration curves were less steep in comparison with those obtained in the assays of IgG or PSA. This is probably because

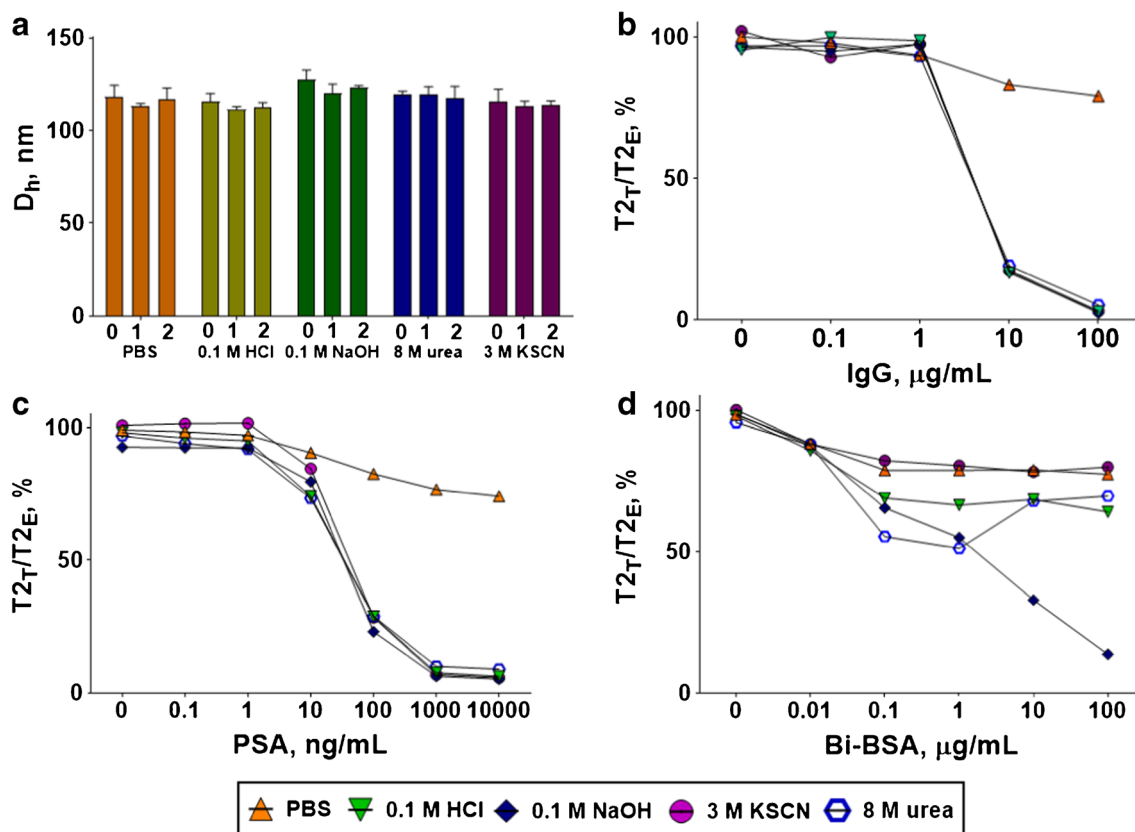


Fig. 2 a Hydrodynamic diameter (D_h) of Fe@C-NH₂/BSA/G in the different elution solutions after 0, 1, and 2 h, $n = 3$. b–d Calibration curves of human IgG, $n = 1$ (b); PSA, $n = 1$ (c), and Bi-BSA, $n = 1$ (d), which were obtained using different elution solutions (legend is at the bottom of the figure)

the rate of protein desorption from the polystyrene plate is slower in comparison with the rate of disruption of the bond between the analyte and recognition molecule (e.g., protein G and IgG). The duration of the elution step was 60 min in all the experiments, and the obvious detachment of the Bi-BSA molecules requires more time to reach saturation. Therefore, 0.1-M NaOH efficiently detaches the magnetic nanoclusters in a sandwich and direct assay, independent of the “analyte-recognition molecule” pair.

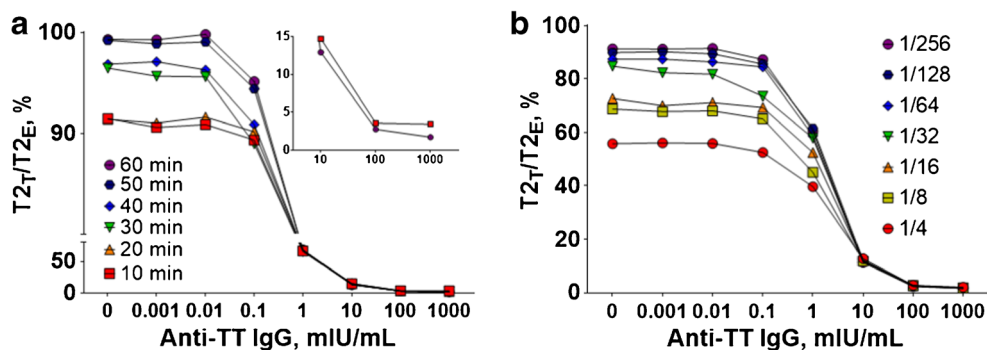
Optimization of the NMR assay of IgG against tetanus toxoid

The indirect assay of human IgG specific to tetanus toxoid (TT) was designed in the subsequent experiments. A 0.1-M NaOH solution was used to detach the nanoclusters from the well surfaces. The level of anti-TT antibodies reflects the protection against tetanus. According to WHO recommendations, 0.1 IU/mL is the protective threshold for in vitro assays (ELISA) [27]. First, the duration of the elution step was optimized. In preliminary experiments, the detachment step was 60 min, but usually less time is necessary to disrupt the bond between the antigen and antibody or between IgG and protein G [22]. We added 0.1-M NaOH to the wells and monitored the

$T2$ in 10 min intervals. As expected, even short exposure to the alkaline solution led to the disruption of the immune complexes (Fig. 3a). Although the 10-min-long elution step provides a calibration curve with a steep slope, we consider that achieving a stable, unchanged $T2$ signal is necessary, because processing the 96-well plate takes several minutes. This time, delay between the measurements of the first and last wells can lead to inaccurate results, especially in samples with low analyte concentrations, in which the change in the $T2$ is more prominent.

A small increase in $T2_T/T2_E$ in samples with a low concentration was a rather unexpected result. Logically, the number of magnetic nanoparticles desorbed from the well’s surface should increase over time and reduce the $T2_T/T2_E$ of the solution. The magnetic nanoparticles used in this work are clusters of Fe@C particles surrounded by a protein shell. Most likely, incubation of nanoparticles in a solution of 0.1-M NaOH could lead to the destruction of some of these nanoclusters or their aggregation. However, the percentage of such nanoparticles is probably small because, otherwise, it would affect their hydrodynamic diameter, and this did not happen (Fig. 2a). We assume that aggregation of a small portion of eluted nanoparticles occurred in all wells. Since the concentration of desorbed nanoparticles (and $T2_T/T2_E$) was

Fig. 3 **a, b** Influence of the elution duration (**a**) or serum dilution (**b**) on the shape of the anti-TT IgG calibration curve, $n = 1$. **a** Inset: T_{2T}/T_{2E} after 10 and 60 min of elution in samples with high antibody concentration. **b** Tenfold dilutions of anti-TT IgG were prepared using negative rabbit serum diluted with the blocking buffer by 1/4, 1/8, 1/16, and so on



minimal in samples with a low IgG concentration, the effect of aggregation of nanoparticles on T_{2T}/T_{2E} , dominated over the effect of desorption; therefore, the increase in T_{2T}/T_{2E} in them was observed. In samples with a high concentration of IgG, effect of nanoparticle desorption was more prominent, and the expected decrease in T_{2T}/T_{2E} occurred after an hour of elution: from 3.8 to 2.9% at an IgG concentration of 100 $\mu\text{g}/\text{mL}$, from 15.8 to 13.9% at an IgG concentration of 10 $\mu\text{g}/\text{mL}$ (Fig. 3a, inset).

Blood serum is a complex medium whose components can affect the performance of an immunoassay (matrix effect). Different concentrations of anti-TT IgG were added to rabbit serum diluted twofold with a blocking buffer. We studied the influence of serum dilution on the shape of the calibration curve and revealed that the best resolution is achieved at dilutions of 1/64 and more (Fig. 3b). The steepest portion of the calibration curve is in the range of anti-TT IgG concentrations between 0.1 and 10 mIU/mL. Considering that the protective threshold is 100 mIU/mL, diluting the serum sample by 1/100 is sufficient for achieving good discrimination between protected and unprotected individuals. Note that rabbit serum was used to establish a calibration curve because we could not

obtain antitoxin-free serum due to the small percentage of seronegative individuals in the population.

The decrease of T_{2T}/T_{2E} in the blood serum samples with a lower dilution (less than 1/64) can be due to two reasons. The first reason is the non-specific sorption of iron-containing serum proteins such as transferrin [28] on the polystyrene surface and their subsequent desorption with an elution solution. Indeed, T_2 of whole pooled human and rabbit serum was 408 ms and 480 ms, respectively, much less than that of water (approximately 2000 ms). With a high dilution of blood serum, the amount of adsorbed iron-containing proteins becomes insignificant and does not affect the sample's T_{2T}/T_{2E} . The second reason is that some serum components are absorbed on the polystyrene surface and interact non-specifically with the conjugate. Most likely, there is a simultaneous influence of both factors.

Interestingly, we previously used a similar analysis format and the same nanoparticles for NMR assay of PSA in blood serum diluted 1/2 on a nitrocellulose membrane. No non-specific interactions were observed. This is probably due to the different chemical structures of polystyrene and nitrocellulose.

Fig. 4 Elemental analysis of elution solutions from positive (100 mIU/mL of anti-TT IgG) and negative (without anti-TT IgG) sample

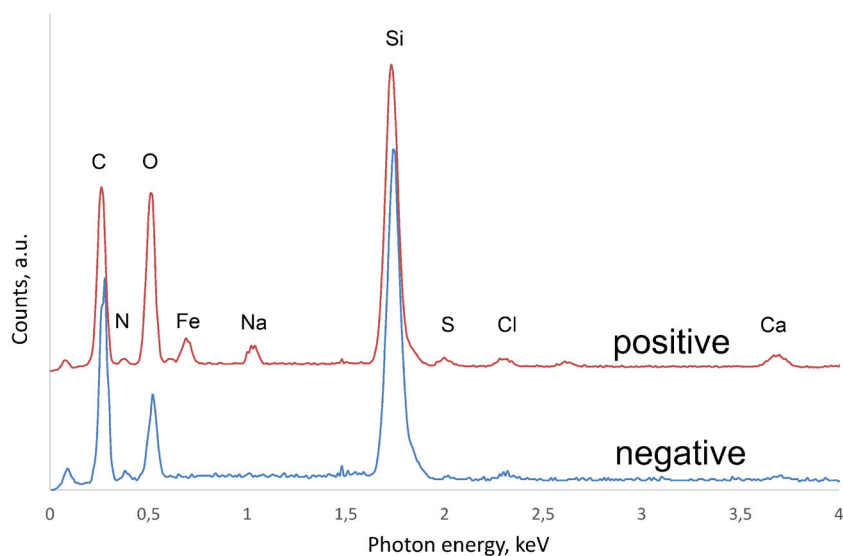


Table 1 Comparison of the immunoassay with known methods of anti-TT IgG detection

Assay	Label	LOD, mIU/mL	Assay duration (without signal measurement), h	Reference
Double-antigen ELISA	Horseradish peroxidase	0.01	4.5	[29]
Multiplex fluorescent immunoassay	Fluorescence microbeads and dyes	0.01	1.25	[30]
Lateral flow assay	Gold nanoparticles	10	0.25	[31]
Localized surface plasmon resonance assay on CDs	Gold nanoparticles	5	2.66	[32]
Indirect ELISA on poly(acrylonitrile) fibers	Horseradish peroxidase	0.5	2.15	[33]
Microfluidic droplet fluorescent assay	Alexa fluor 488	100	Less than 1	[34]
NMR relaxometry	Carbon-coated iron nanoparticles	0.08–0.12	3	This work

Decrease of T2 is caused by detached magnetic nanoparticles

To confirm that the elution of iron-carbon nanoparticles causes the changes in relaxation time, we estimated the iron content in elution solutions of positive and negative samples (with and without anti-TT IgG) by elemental analysis. Due to the meager amount of iron in a single positive sample, we combined and concentrated elution solutions from 24 wells for both positive and negative samples. Mean T2 of positive samples was 105 ms; mean T2 of negative samples was 2023 ms. Relaxation times of combined positive and negative samples after dialysis were 106 and 2001 ms, respectively, indicating that the source of T2 decrease cannot pass through pores of dialysis tubing with 10 kDa molecular weight cutoff. After dialysis, both samples were concentrated at 95 °C to 100–200 µL and were visually different. The positive sample contained micrometer-scale black aggregates; the negative sample was clear.

Dried samples were analyzed by SEM (see Supplementary Information (ESM) Fig. S1) and EDAX using the “create max pixel spectrum” procedure of EDAX Team software to search the low-concentration elements. This procedure searches through all the pixels in the recorded map for each energy channel and finds the pixel that has the maximum count for that energy. The generated spectrum shows the highest count numbers for each energy channel. In the positive sample, iron at 0.705 keV was detected (Fig. 4). Although traces of iron

were found in the negative sample, iron concentration is significantly higher in the positive sample. Notably, Na, Cl, Ca, and S concentrations were also higher in the positive sample, resulting from incomplete dialysis and the presence of NaCl and casein (casein micelles usually contain Ca). We suppose that black aggregates found in concentrated positive sample were clumped nanoparticles or casein residues (or both).

Performance of anti-TT IgG NMR assay

The calibration curves were generated by fitting the measured data to a logistic function (adjusted parameters can be found in ESM, Table S1). The analytical sensitivity of the immunoassay (lower limit of detection, LOD) varied from day to day and was from 0.08 to 0.12 mIU/mL. Thus, the LOD of NMR analysis based on magnetic nanoparticle elution is 4–7 times lower than that of the previously developed NMR analysis on a nitrocellulose membrane (0.52 mIU/mL) [12]. The capacity of protein sorption on the surface of polystyrene plates does not exceed 1 µg/cm², while the nitrocellulose membrane’s capacity is much higher: about 150 µg/cm². Both assays were identical to the reagents used and the conditions of the analysis (the duration of incubation steps and temperature). Thus, we believe that the increased detection sensitivity is because of the detachment of the magnetic nanoparticles from the solid phase and larger sample volume. The analytical sensitivity of the immunoassay allows for the quantification of tetanus antitoxin in 100-fold diluted serum samples. The LOD of the assay is 8 times higher than that of ELISA and bead-based fluorescent

Table 2 Spike-recovery test and NMR assay reproducibility, *n* = 10

Expected concentration, IU/mL	Measured concentration, IU/mL	Recovery, %	CV, %
0.2	0.338	169	7.411
1.3	1.372	109.8	6.188
2	3.001	150.1	4.163
3	2.972	118.9	6.561
5	5.614	112.3	1.723
10	12.36	123.6	2.817
50	52.12	104.2	4.061
80	80.704	100.88	6.1963

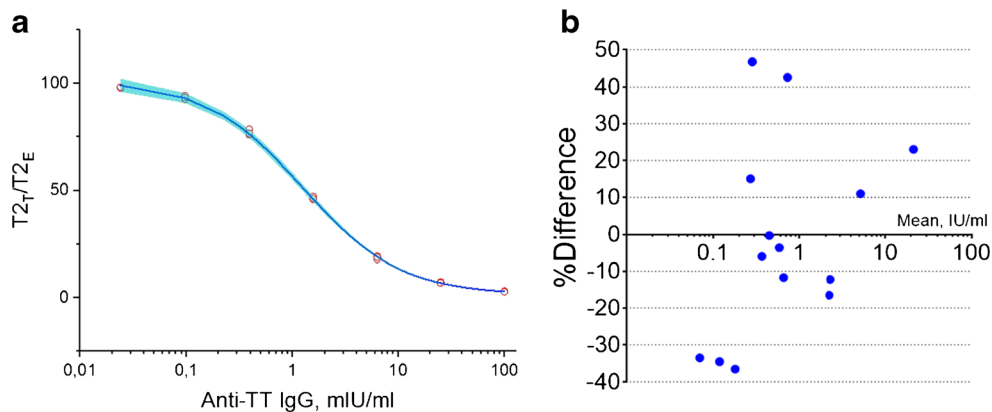


Fig. 5 **a** Representative anti-TT IgG calibration plot obtained using the negative rabbit serum diluted by 1/100 in the blocking buffer as the sample matrix, $n=3$, data points are presented. The blue area between 95% CI bands is the area that contains the true calibration curve with 95% probability. **b** Bland-Altman plot comparing NMR assay and ELISA. X-

axis—mean of anti-TT IgG concentrations measured by NMR assay and ELISA. Y-axis—the difference between concentrations measured by NMR assay and ELISA divided by the average concentration measured by both methods (in percent)

assays but is lower in comparison with other immunoassays described in the literature (Table 1).

In order to assess the assay accuracy and precision, the negative serum was spiked with different amounts of anti-TT IgG. Totally, eight samples (10 replications per sample) with concentrations from 0.2 to 80 mIU/mL were tested. The IgG concentrations in the spiked samples were back-calculated using the calibration curve; then, the coefficient of variation (CV) was estimated for each sample. In all the samples, the CV did not exceed 7.4% (Table 2), which is within the acceptable range ($<15\%$) [35]. The recovery was within the acceptable limits ($\pm 20\%$) for 5 of 8 tested concentrations (Table 2) [35]. In all cases, the recovery value was higher than 100%. At a concentration of 0.2 mIU/mL, recovery was as high as 169%. This concentration is close to the LOD; moreover, as can be seen from the calibration curve (Fig. 5a), fitting was less reliable in the range of low anti-TT IgG. We can explain the poor recovery of 2 and 10 mIU/mL samples only by dilution errors because recovery of neighbor concentrations was within acceptable limits.

We evaluated tetanus IgG concentration in 15 blood serums obtained from volunteers using commercial ELISA and NMR analysis (see ESM, Table S2). The results are presented in Fig. 5b as a Bland-Altman plot. For some serums, ELISA showed a higher concentration, for some—NMR assay. The Bland-Altman analysis showed no relevant bias between both methods: on average, IgG concentrations measured by ELISA were only 1% higher (bias: -1.185% , 95% CI from -53.09 to 50.71%). However, for individual serums, differences in IgG concentrations were up to 50%. Note that serum from a non-vaccinated person was excluded from comparative analysis due to antibody concentration below the NMR assay detection limit. We compared the results with data from other authors and found that differences of the same order are observed even when comparing two tetanus IgG

assays from the same manufacturer (see Fig. 3 in ref. [36]). In the ELISA, the tetanus toxin is used as a coating antigen. On the other hand, when developing NMR assay, we coated the wells with tetanus toxoid. Tetanus toxoid is produced by inactivating the toxin with formaldehyde. Toxoid lacks toxicity but retains immunogenicity. An indirect enzyme-linked immunosorbent assay in which tetanus toxoid was used as the coating antigen correlated well with the neutralization reaction in which tetanus toxin was used [37]. However, tetanus toxoid possesses several unique epitopes [38, 39]. Moreover, the same monoclonal antibody can have different reactivity towards toxin and toxoid [39]. Therefore, the inconsistencies in the results of NMR assay and ELISA can be explained by the different affinities of anti-TT IgG to tetanus toxin and toxoid.

Conclusion

We designed an NMR immunoassay, whose main feature is the displacement of nanomagnetic labels from the solid phase to the solution, which allows for the sensitive detection of the analyte. The applicability of the developed NMR assay was demonstrated by detecting biotinylated protein, PSA, and human IgG against tetanus toxoid. Measurement of T2 in the volume allowed 4–7 times LOD decrease for anti-TT IgG compared to the analysis of the same format on a porous membrane.

The assay is performed in 96-well plates and is thus compatible with general analytical laboratory equipment, including pipettes, washers, and dispensers. Therefore, most of the assay steps can be automated. All the reagents necessary for the immunoassay are also common, except for the conjugates of the magnetic nanoparticles. In this work, we used functionalized carbon-coated iron nanoparticles, which are not

commercially available. However, any other magnetic nanomaterials with high relaxivities and that are stable in elution solutions can be used as labels. For example, conjugates of iron oxide nanoparticles possessing high relaxivities can be prepared in a relatively simple manner with a wide variety of coatings and conjugation chemistries [40]. Commonly available Dynabeads or any commercial magnetic nano-/microparticles are another possible option. We should note that the properties of the magnetic nanomaterial will affect the performance of the NMR immunoassay, and optimizations will be necessary.

Disadvantages of the NMR immunoassay are the limited availability of NMR relaxometers and time-consuming measurement procedure. Relaxometers are not common instruments in biomedical laboratories, but according to a recent report [41], desktop and mobile platforms are expected to be more available for consumers in the near future. The simplification of the T2 measurements is another direction for improvements. Herein, we broke off wells of well plates, which were then put inside an RF coil to measure the T2. The single measurement by itself takes less than 1 min, but manually processing the whole 96-well plate is tedious. There are two ways to overcome this disadvantage. The first method is the development of relaxometers that are capable of measuring several samples simultaneously [42]. The second way is the application of a device that will place the wells of the well plate inside the RF coil automatically.

Supplementary Information The online version contains supplementary material available at <https://doi.org/10.1007/s00216-020-03112-7>.

Funding information This work was supported by the Russian Science Foundation (Grant No. 17-15-01116).

Compliance with ethical standards

Conflict of interest The authors declare that they have no conflict of interest.

Research involving human participants and/or animals All procedures performed in studies involving human participants were in accordance with the 1964 Declaration of Helsinki and its later amendments or comparable ethical standards. Research was approved by the Review Board of the Institute of Ecology and Genetics of Microorganisms UB RAS (IRB00010009).

Informed consent Written informed consent was obtained from volunteers.

References

- Alcantara D, Lopez S, García-Martin ML, Pozo D. Iron oxide nanoparticles as magnetic relaxation switching (MRSw) sensors: current applications in nanomedicine. *Nanomedicine*. 2016;12:1253–62. <https://doi.org/10.1016/j.nano.2016.01.005>.
- Kim J, Mohamed MAA, Zagorovsky K, Chan WCW. State of diagnosing infectious pathogens using colloidal nanomaterials. *Biomaterials*. 2017;146:97–114. <https://doi.org/10.1016/j.biomaterials.2017.08.013>.
- Denmark DJ, Bustos-Perez X, Swain A, Phan MH, Mohapatra S, Mohapatra SS. Readiness of magnetic nanobiosensors for point-of-care commercialization. *J Electron Mater*. 2019;48:4749–61. <https://doi.org/10.1007/s11664-019-07275-7>.
- Huang Z, Hu S, Xiong Y, Wei H, Xu H, Duan H, et al. Application and development of superparamagnetic nanoparticles in sample pretreatment and immunochromatographic assay. *Trends Anal Chem*. 2019;114:151–70. <https://doi.org/10.1016/j.trac.2019.03.004>.
- Knežević NŽ, Gadjanski I, Durand JO. Magnetic nanoarchitectures for cancer sensing, imaging and therapy. *J Mater Chem B*. 2019;7:9–23. <https://doi.org/10.1039/c8tb02741b>.
- Nabaei V, Chandrawati R, Heidari H. Magnetic biosensors: modeling and simulation. *Biosens Bioelectron*. 2018;103:69–86. <https://doi.org/10.1016/j.bios.2017.12.023>.
- Yang J, Wang K, Xu H, Yan W, Jin Q, Cui D. Detection platforms for point-of-care testing based on colorimetric, luminescent and magnetic assays: a review. *Talanta*. 2019;202:96–110. <https://doi.org/10.1016/j.talanta.2019.04.054>.
- Zhang Y, Yang H, Zhou Z, Huang K, Yang S, Han G. Recent advances on magnetic relaxation switching assay-based nanosensors. *Bioconjug Chem*. 2017;28:869–79. <https://doi.org/10.1021/acs.bioconjchem.7b00059>.
- Ullman E. Homogeneous immunoassays. In: Wild D, editor. *The immunoassay handbook*. Amsterdam: Elsevier Science; 2013. p. 67–87.
- Burtea C, Laurent S, Mahieu I, Larbanoix L, Roch A, Port M, et al. In vitro biomedical applications of functionalized iron oxide nanoparticles, including those not related to magnetic properties. *Contrast Media Mol Imaging*. 2011;6:236–50. <https://doi.org/10.1002/cmmi.423>.
- Khramtsov P, Kropaneva M, Bochkova M, Timganova V, Zamorina S, Rayev M. Solid-phase nuclear magnetic resonance immunoassay for the prostate-specific antigen by using protein-coated magnetic nanoparticles. *Microchim Acta*. 2019;186:768. <https://doi.org/10.1007/s00604-019-3925-4>.
- Khramtsov P, Barkina I, Kropaneva M, Bochkova M, Timganova V, Nechaev A, et al. Magnetic nanoclusters coated with albumin, casein, and gelatin: size tuning, relaxivity, stability, protein corona, and application in nuclear magnetic resonance immunoassay. *Nanomaterials*. 2019;9:1345. <https://doi.org/10.3390/nano9091345>.
- Piletsky SS, Cass AEG, Piletska EV, Czulak J, Piletsky SA. A novel assay format as an alternative to ELISA: MINA test for biotin. *ChemNanoMat*. 2018;4:1214–22. <https://doi.org/10.1002/cnma.201800393>.
- Mao X, Jiang J, Chen J, Huang Y, Shen G, Yu R. Cyclic accumulation of nanoparticles: a new strategy for electrochemical immunoassay based on the reversible reaction between dethiobiotin and avidin. *Anal Chim Acta*. 2006;557:159–63. <https://doi.org/10.1016/j.aca.2005.09.078>.
- Glass JR, Dickerson JC, Schultz DA. Enzyme-mediated individual nanoparticle release assay. *Anal Biochem*. 2006;353:209–16. <https://doi.org/10.1016/j.ab.2006.03.020>.
- Lin Y, Zhou Q, Lin Y, Tang D, Chen G, Tang D. Simple and sensitive detection of aflatoxin B1 within five minute using a non-conventional competitive immunosensing mode. *Biosens Bioelectron*. 2015;74:680–6. <https://doi.org/10.1016/j.bios.2015.07.029>.
- Takae S, Akiyama Y, Yamasaki Y, Nagasaki Y, Kataoka K. Colloidal Au replacement assay for highly sensitive quantification of low molecular weight analytes by surface plasmon resonance.

- Bioconjug Chem. 2007;18:1241–5. <https://doi.org/10.1021/bc0603541>.
18. Halonen S, Kangas T, Haataja M, Lassi U. Urea-water-solution properties: density, viscosity, and surface tension in an under-saturated solution. *Emiss Control Sci Technol*. 2017;3:161–70. <https://doi.org/10.1007/s40825-016-0051-1Y.K>.
 19. Agrawal YK, Sabbagh R, Sanders S, Nobes DS. Measuring the refractive index, density, viscosity, pH, and surface tension of potassium thiocyanate (KSCN) solutions for refractive index matching in flow experiments. *J Chem Eng Data*. 2018;63:1275–85. <https://doi.org/10.1021/acs.jced.7b00904>.
 20. Warren JR, Gordon JA. On the refractive indices of aqueous solutions of urea. *J Phys Chem*. 1966;70:297–300. <https://doi.org/10.1021/j100873a507>.
 21. Ayyar BV, Arora S, Murphy C, O’Kennedy R. Affinity chromatography as a tool for antibody purification. *Methods*. 2012;56:116–29. <https://doi.org/10.1016/j.ymeth.2011.10.007>.
 22. Yan Z, Huang J. Chromatographic behavior of mouse serum immunoglobulin G in protein G perfusion affinity chromatography. *Chromatogr B Biomed Sci Appl*. 2000;738:149–54. [https://doi.org/10.1016/S0378-4347\(99\)00507-1](https://doi.org/10.1016/S0378-4347(99)00507-1).
 23. Acevedo B, Perera Y, Torres E, Pentón D, Ayala M, Gavilondo J. Fast and novel purification method to obtain the prostate specific antigen (PSA) from human seminal plasma. *Prostate*. 2006;66:1029–36. <https://doi.org/10.1002/pros.20267>.
 24. Fahmi MZ, Ou K, Chen JK, Ho MH, Tzing SH, Chang JY. Development of bovine serum albumin-modified hybrid nanoclusters for magnetofluorescence imaging and drug delivery. *RSC Adv*. 2014;4:32762–72. <https://doi.org/10.1039/c4ra05785f>.
 25. Strozyk MS, Chanana M, Pastoriza-Santos I, Pérez-Juste J, Liz-Marzán LM. Protein/polymer-based dual-responsive gold nanoparticles with pH-dependent thermal sensitivity. *Adv Funct Mater*. 2012;22:1436–44. <https://doi.org/10.1002/adfm.201102471>.
 26. Rybak JN, Scheurer SB, Neri D, Elia G. Purification of biotinylated proteins on streptavidin resin: a protocol for quantitative elution. *Proteomics*. 2004;4:2296–9. <https://doi.org/10.1002/pmic.200300780>.
 27. Yen LM, Thwaites CL. Tetanus. *Lancet*. 2019;393:1657–68. [https://doi.org/10.1016/S0140-6736\(18\)33131-3](https://doi.org/10.1016/S0140-6736(18)33131-3).
 28. Yilmaz A, Ulak FŞ, Batun MS. Proton T1 and T2 relaxivities of serum proteins. *Magn Reson Imaging*. 2004;22:683–8. <https://doi.org/10.1016/j.mri.2004.02.001>.
 29. Kristiansen M, Aggerbeck H, Heron I. Improved ELISA for determination of anti-diphtheria and/or anti-tetanus antitoxin antibodies in sera. *APMIS*. 1997;105:843–53.
 30. van Gageldonk PGM, van Schaijk FG, van der Klis FR, Berbers GAM. Development and validation of a multiplex immunoassay for the simultaneous determination of serum antibodies to *Bordetella pertussis*, diphtheria and tetanus. *J Immunol Methods*. 2008;335:79–89. <https://doi.org/10.1016/j.jim.2008.02.018>.
 31. Liu J, Wang J, Li Z, Meng H, Zhang L, Wang H, et al. A lateral flow assay for the determination of human tetanus antibody in whole blood by using gold nanoparticle labeled tetanus antigen. *Microchim Acta*. 2018;185:110. <https://doi.org/10.1007/s00604-017-2657-6>.
 32. Raeisi S, Molaeirad A, Sadri M, Nejad HR. Detection of anti-tetanus toxoid monoclonal antibody by using modified polycarbonate surface. *Plasmonics*. 2018;13:1555–67. <https://doi.org/10.1007/s11468-017-0664-4>.
 33. Jain S, Chattopadhyay S, Jackeray R, Zainul Abid CKV, Kumar M, Singh H. Detection of anti-tetanus toxoid antibody on modified polyacrylonitrile fibers. *Talanta*. 2010;82:1876–83. <https://doi.org/10.1016/j.talanta.2010.08.003>.
 34. Golberg A, Yarmush ML, Konry T. Picoliter droplet microfluidic immunosorbent platform for point-of-care diagnostics of tetanus. *Microchim Acta*. 2013;180:855–60. <https://doi.org/10.1007/s00604-013-0998-3>.
 35. Bioanalytical Method Validation. FDA. 2018. <https://www.fda.gov/media/70858/download>. Accessed 29 Oct 2019.
 36. Reder S, Riffelmann M, Becker C, Wirsing von König CH. Measuring immunoglobulin G antibodies to tetanus toxin, diphtheria toxin, and pertussis toxin with single-antigen enzyme-linked immunosorbent assays and a bead-based multiplex assay. *Clin Vaccine Immunol*. 2008;15:744–9. <https://doi.org/10.1128/CVI.00225-07>.
 37. Manghi MA, Pasetti MF, Brero ML, Deluchi S, di Paola G, Mathet V, et al. Development of an ELISA for measuring the activity of tetanus toxoid in vaccines and comparison with the toxin neutralization test in mice. *J Immunol Methods*. 1994;168:17–24. [https://doi.org/10.1016/0022-1759\(94\)90204-6](https://doi.org/10.1016/0022-1759(94)90204-6).
 38. Ahnert-Hilger G, Bizzini B, Goretzki K, Müller H, Völckers C, Habermann E. Monoclonal antibodies against tetanus toxin and toxoid. *Med Microbiol Immunol*. 1983;172:123–35. <https://doi.org/10.1007/BF02124513>.
 39. Volk WA, Bizzini B, Snyder RM, Bernhard E, Wagner RR. Neutralization of tetanus toxin by distinct monoclonal antibodies binding to multiple epitopes on the toxin molecule. *Infect Immun*. 1984;45:604–9. <https://doi.org/10.1128/iai.45.3.604-609.1984>.
 40. Kaittanis C, Santra S, Santiesteban OJ, Henderson TJ, Perez JM. The assembly state between magnetic nanosensors and their targets orchestrates their magnetic relaxation response. *J Am Chem Soc*. 2011;133:3668–76. <https://doi.org/10.1021/ja1109584>.
 41. Blümich B. Low-field and benchtop NMR. *J Magn Reson*. 2019;306:27–35. <https://doi.org/10.1016/j.jmr.2019.07.030>.
 42. Huber S, Min C, Staat C, Oh J, Castro CM, Haase A, et al. Multichannel digital heteronuclear magnetic resonance biosensor. *Biosens Bioelectron*. 2019;126:240–8. <https://doi.org/10.1016/j.bios.2018.10.052>.

Publisher’s note Springer Nature remains neutral with regard to jurisdictional claims in published maps and institutional affiliations.